Regular Article

PHYSICAL CHEMISTRY RESEARCH
Published by the
Iranian Chemical Society
www.physchemres.org
info@physchemres.org

Phys. Chem. Res., Vol. 6, No. 4, 857-869, December 2018
DOI: 10.22036/pcr.2018.145269.1528

Molecular Development of Silver Nanoparticles-loaded Poly Acrylic Acid Hydrogel as a Catalyst for Dye Degradation

A. Heidari[a], H. Moghimi[b], J. Rashidiani[a] and R.A. Taheri[a,*]

[a]*Nanobiotechnology Research Center, Baqiyatallah University of Medical Sciences, Tehran, Iran*

[b]*Department of Microbial Biotechnology, School of Biology, College of Science, University of Tehran, Tehran, Iran*

(Received 23 August 2018, Accepted 7 October 2018)

In this study, Ag nanoparticles were loaded successfully into poly acrylic acid hydrogel (PAA) as a matrix to prepare PAA-Ag nanocomposite catalyst. The prepared catalyst was characterized by scanning electron microscope (SEM), transmission electron microscope (TEM), Fourier transform infrared spectrophotometer (FT-IR), thermal gravimetric analyzer (TGA), inductively coupled plasma atomic emission spectrometer (ICP), and X-Ray photoelectron spectroscope (XPS). The catalyst with $NaBH_4$ was used to degrade some common pollutant dyes such as methyl orange (MO), rhodamine B (Rh. B) and methylene blue (MB) in water. UV-visible spectrophotometer was applied to determine the initial and final concentration of dyes. Some effective factors on degradation such as the amount of catalyst, the initial concentration of dye, time, and pH were investigated. The results demonstrated that the amount of catalyst equal to 0.02 and 0.03 g with 0.01 g of $NaBH_4$ in 50 ml water are appropriate to completely degrade 50 ppm of MO, Rh. B, and MB, respectively, at pH = 6.5 in less than 15 min.

Keywords: Degradation, Electron relay effect, Poly acrylic acid hydrogel, Silver nanoparticle, Methyl orange, Methylene blue, Rhodamine B, Dye

Abbreviations: Acrylic acid (AA), Ammonium persulfate (APS), Fourier transform infrared spectrophotometer (FT-IR), Inductively coupled plasma atomic emission spectrometer (ICP), Methylene blue (MB), N, N′-methylene bis-acrylamide (MBA), Methyl orange (MO), Nanoparticles (NPs), Poly acrylic acid hydrogel (PAA), Silver nanoparticles loaded poly acrylic acid nanocomposite (PAA-Ag), Rhodamine B (Rh. B), Scanning electron microscope (SEM), Transmission electron microscope (TEM), N,N,N′,N′-tetra methyl methylene di amine (TEMED), Thermal gravimetric analyzer (TGA), X-Ray photoelectron spectroscope (XPS).

INTRODUCTION

Due to rapid industrialization and urbanization, organic dyes have become one of the main sources of severe pollutions in wastewaters [1,2]. Organic dyes discharged from different industries such as textile, paper, printing, food, and cosmetic industries to our surrounding water bodies result in significant environmental pollution [3,4]. Dye effluents color water bodies and disturb the natural growth activity of aquatic life by decreasing the dissolved oxygen of water [5]. Likewise, they can cause human injuries such as eye irritation, skin irritation, multi-organ tissue injury, several cancers, and lung disease [6,7]. Consequently, the removal and/or reduction of organic hazardous dye effluents, for instance, methyl orange (MO), methylene blue (MB), and rhodamine B (Rh. B), in wastewater is a demanding effort. In this regard, conventional biological treatment, like using microorganisms [8,9], and also typical wastewater treatment methods including adsorption [10], photocatalytic degradation [11], chemical oxidation [12], membrane filtration [13,14], flocculation [15] and electro-oxidation

*Corresponding author. E-mail: taheri@bmsu.ac.ir

[16,17] have been documented for reduction of organic dyes. However, they are generally ineffective methods because dye effluents are highly resistant to microorganisms. In this respect, the assessments performed showed that activated carbon adsorption and coagulation technologies are not effective. In addition, oxidation technique produces by-products that might be toxic [14]. Furthermore, dye destruction by means of physical-chemical treatments in a high effluent concentration is practically impossible.

In order to solve these issues, nanotechnology recently has been extended to the wastewater treatments [9,18]. Due to the high surface area of nanoparticles that exhibit enhanced reactivity, they have many promising applications in effluent treatments [19-21]. Silver nanoparticles (Ag NPs) along with many applications ranging from sensing to optics [22,23], data storage and antibacterial activity [24-26] act as the suitable catalysts in water treatment [27-29]. Ag NPs possesses excellent electron relay effect [30] than the other transition elements, as a main advantage. In addition, the Ag nanoparticles have superior anti-bacterial properties [31]. In spite of many advantages, Ag NPs suffer from instability in water and tend to aggregate which in the long run decreases their catalysts ability. To protect Ag NPs from aggregation, both electrostatic and steric stabilization methods have been used [32-34]. Among all of the stabilizing systems, hydrogels are the most powerful ones, particularly when stabilized metal nanoparticles are used as catalysts. Hydrogels provide large free space between the cross-linked networks that act as a nanoreactor for the nucleation and growth of the nanoparticles [35-37]. Moreover, the surface of the metal nanoparticles not only is not affected by stabilization, but also the speed of catalytic reaction can be tuned by controlling the crosslinking density of the polymeric network.

This paper aims at studying the ability of synthesized Ag-NPs as an efficient catalyst for the degradation of organic dye pollutants such as MB, Rh. B and MO using $NaBH_4$ as a reducing agent at room temperature.

According to the best of our knowledge, this is for the very first time that Ag-NPs fabricated in PAA hydrogel are being used as the catalyst with high activity toward methylene blue (MB), methyl orange (MO), and rhodamine B (Rh. B) in current approach. Among the various kinds of PAA-based catalysts, the applied approach in this study showed excellent results for the degradation of dyes compared to other similar studies in the literature. The effect of various parameters on the dye reduction was studied. The reusability of the catalyst was also investigated for three consecutive cycles.

EXPERIMENTAL

Materials

Acrylic acid (AA), ammonium persulfate (APS), and methyl orange (MO) were supplied by Sigma Aldrich. N,N′-methylene bis-acrylamide (MBA) and the N,N,N′,N′-tetra methyl methylene di amine (TEMED) were obtained from Acros. Hydrochloric acid (HCl), sodium hydroxide (NaOH), Ag (CH_3COO), sodium borohydride ($NaBH_4$), methylene blue (MB), and rhodamine B (Rh. B) were purchased from Merck. All samples were used without further purification. All solutions were prepared using deionized water throughout the experiments.

Instrumentation

A Bruker FT-IR spectrophotometer was used to record FT-IR spectra in KBr disk. ICP-AES, Spectro Genesis was applied to determine the amount of loaded silver in PAA hydrogel. Scanning electron microscopy (SEM), MIRA3 FEG SEM (Tescan, Czech Republic), was utilized to investigate the morphology of PAA hydrogel by accelerating voltage equal to 10 keV. The size and nanostructure of silver NPs inside the PAA-Ag nanocomposite was characterized by transmission electron microcopy (TEM, HITACHI S-4800). Thermogravimetric analysis (TGA) was carried out to study the thermal properties of PAA-Ag nanocomposite by an STA409PC Netzsch thermal analyzer, made in Germany. The X-ray photoelectron spectrum (XPS) was performed by a 1600E Perkin Elmer applying Mg-K_α excitation source. UV-visible spectra were measured using an Analytik Jena (SPECORD 205) model of UV-Vis double beam spectrophotometer at a wavelength of 200-700 nm. The sample measurements were performed in a 1 cm quartz cuvette at room temperature. Deionized water was used for the background correction of all UV-Vis absorption spectra. The effect of the pH on dye degradation was investigated by pH meter (Metrohm,

Switzerland).

Preparation of Catalyst

Preparation of hydrogel-based AA. 72.5 mmol AA, 55 mg MBA (0.5%) and 10 µl TEMED were mixed with 4 ml of pure water, and then 0.165 g APS dissolved in 1 ml water was added to this solution. Thereafter, it was immersed in a 40 °C water bath for 4 h. Finally, it washed with water to remove un-reacted species and was dried at 40 °C.

In situ synthesis of silver nanoparticles within PAA hydrogel. Silver ions were loaded into the hydrogel network for 24 h at room temperature under continuous stirring. Then, metal ions loaded in hydrogels were treated with 50 ml, 0.1 M $NaBH_4$ as a reducing agent, to reduce the Ag^+ ions to Ag° in the PAA lattice. Finally, the prepared PAA-Ag hydrogel nanocomposites were filtered, and then washed with deionized water.

Catalytic Activity Measurement

The removal of methylene blue (MB, 50 mg l^{-1}), methyl orange (MO, 30 mg l^{-1}) and rhodamine B (Rh. B, 50 mg l^{-1}) in aqueous solution was carried out in the presence of PAA-Ag and $NaBH_4$ as the reducing agent. For this purpose, 0.02 g of the sample was dispersed in 50 ml solution of the dye. The solute on samples was withdrawn from the reaction medium at the regular time intervals. The PAA-Ag was separated from the solution by centrifugation at 4000 rpm for 20 min and the change on the absorbance at a maximum wavelength (λ_{max}) of dyes (664 nm for MB, 462 for MO and 552 nm for Rh. B) was monitored by UV-Vis spectrophotometer. The effect of PAA-Ag amount on the dye removal was studied by contacting 50 ml of dye solution (50 mg l^{-1} for MB and Rh. B and 30 mg l^{-1} for MO) for 60 min. Different amounts of PAA-Ag (0.01, 0.02, 0.03 and 0.04 g) were applied. The effect of initial dye concentration on the dye removal was investigated. The PAA-Ag (0.02 g) was added to 50 ml of different dye concentrations (20, 30, 40 and 50 mg l^{-1} for MB, Rh. B) and (5, 10, 20 and 30 mg l^{-1} for BR5). The effect of various pHs (2, 5, 8 and 9) on the dye removal was studied. The removal performance of the process was defined as:

$$\%\,\mathrm{Re}moval = \frac{(C_0 - C)}{C_0} \times 100 = \frac{(A_0 - A)}{A_0} \times 100 \quad (1)$$

where A_0 and C_0 are the initial absorbance and concentration, A and C are the final absorbance and concentration at λ_{max} = 664 nm for MB, λ_{max}= 462 nm for MO and λ_{max} = 552 nm for Rh. B, respectively.

RESULTS AND DISCUSSION

Characterization

Figure 1 shows the FT-IR spectra of AA, PAA hydrogel, and Ag-PAA nanocomposite. In the figure, the peak at 3530 cm^{-1} is related to OH stretching band and the peaks at 2865 and 2935 cm^{-1} are related to CH stretching bands of AA and PAA hydrogel. Furthermore, CO double bond and COO^- stretching bonds are seen at the 1462 and 1739 cm^{-1} regions, respectively (Boruah *et al.* 2014). In addition, the overlap of OH band and NH band of MBA is seen at about 3200 cm^{-1} [38]. The peak appeared at 400-700 cm^{-1} is assigned to the vibrational bond of the Ag-O in the Ag-PPA lattice. Obviously, this peak is not seen in the FT-IR spectrum of bare PAA. To investigate the morphology of the hydrogel, the SEM analysis was performed. Figure 2 displays the micrographs of the PAA hydrogel that show the highly porous structure of the hydrogel. According to the micrographs, the shape and size of pores were non-uniform. Thermal gravimetric analysis (TGA) was applied to characterize the thermal properties of PAA and PAA-Ag and total amount of entrapped Ag inside the PAA-Ag nanocomposite.

Figure 3 illustrates TGA curves of PAA hydrogel and PAA-Ag nanocomposite. As obviously seen, two weight loss processes occur for both samples while heating up. At the first step, less than 250 °C, the physically absorbed water molecules are realized. At the second step, as the major weight loss, the PAA hydrogel starts to decompose from 250 °C and then are completely decomposed at 800 °C with no carbon residue according to the previously reported research. Comparing the PAA hydrogel and PAA-Ag nanocomposite indicates that total weight ratio of Ag within the PAA-Ag nanocomposite had been 19.7%. It was also

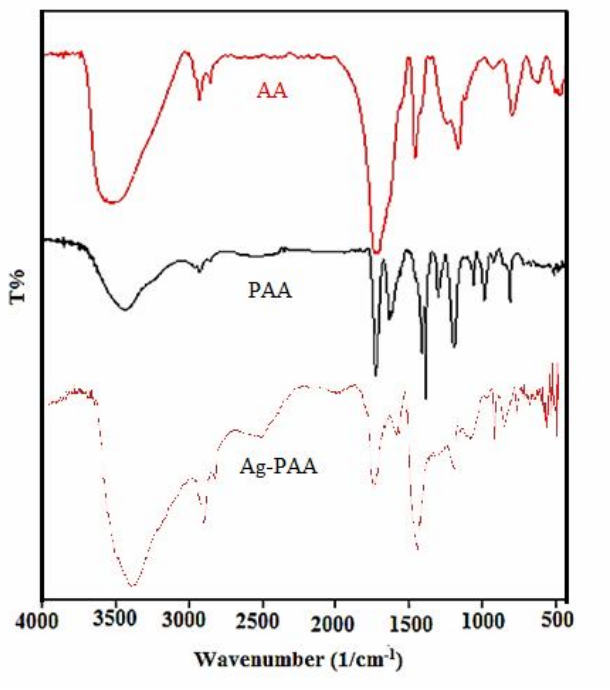

Fig. 1. FT-IR spectra of acrylic acid (AA), poly acrylic acid hydrogel (PAA) and Ag-PAA nanocomposite.

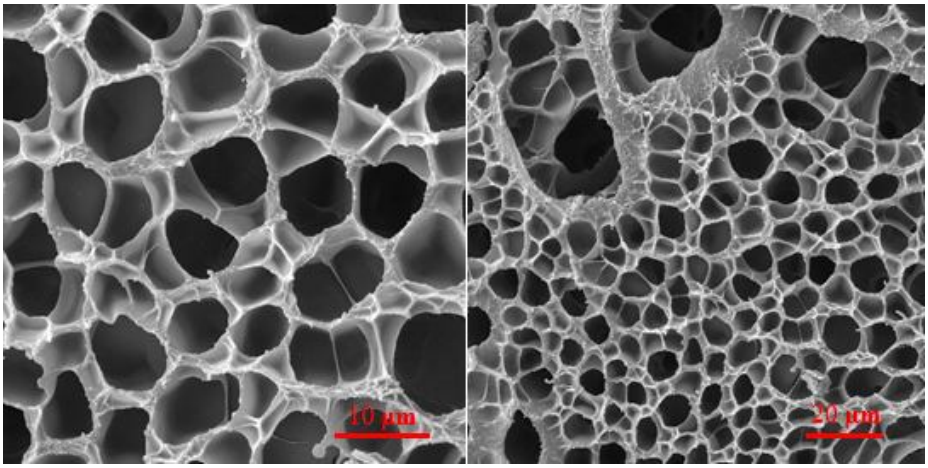

Fig. 2. SEM images of PAA hydrogel.

determined by ICP measurement that displayed Ag weight had been 194 mg within 0.1 g of PAA. In comparison to bare PAA hydrogel, it was obvious that the thermal stability of PAA-Ag nanocomposite has been increased. The stability could be attributed to the formation of coordination bond between Ag NPs and functional group of PPA. The TGA analyses were carried out under N_2 gas to remove the possibility of formation of oxide compounds during the experiment due to the presence of O_2. The formation of oxide could lead to the thermal stability at TGA

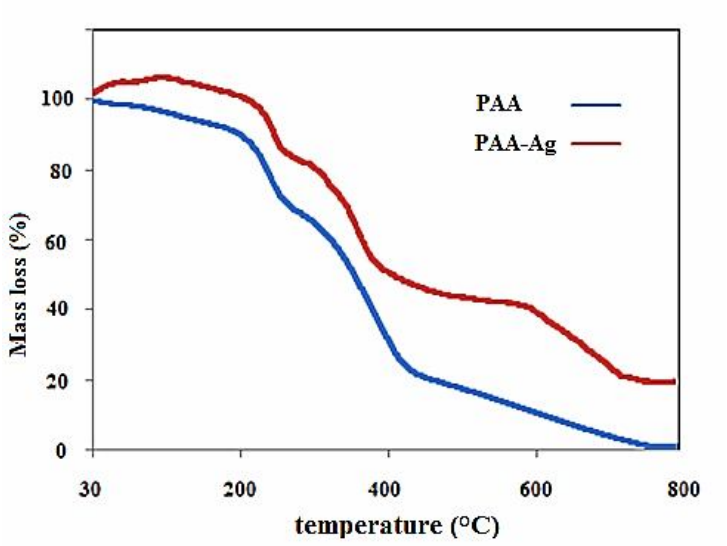

Fig. 3. TGA thermograms of PAA hydrogel and PAA-Ag nanocomposite.

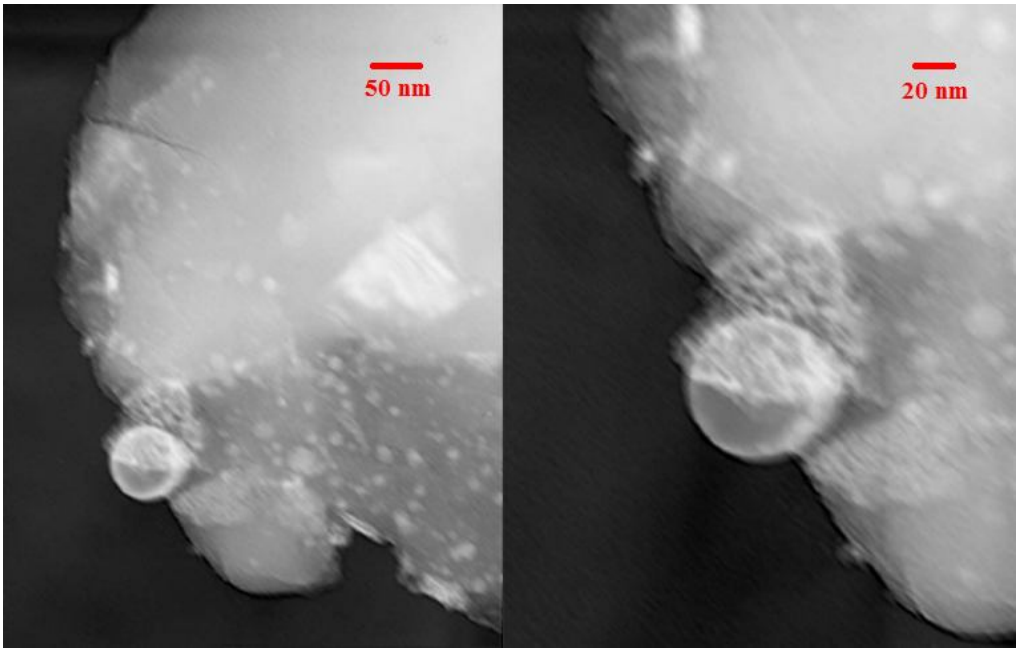

Fig. 4. TEM images of Ag nanoparticle within PAA-Ag nanocomposite.

experiments. The TEM analysis was applied to investigate the nanostructure of PAA-Ag hydrogel (Fig. 4). As shown in Fig. 4, Ag NPs are distributed in PAA matrix and possess spherical shape with sizes about 20-40 nm. The X-ray photoelectron spectroscopy (XPS) was performed to achieve more information about the ionic state of the Ag NPs within the PAA-Ag nanocomposite.

Figure 5 shows a high-resolution Ag XP-spectrum related to the Ag NPs. The observed peaks at 369.95 and 375.97 eV, are related to $3d_{5/2}$ and $3d_{3/2}$ spin-orbit coupled

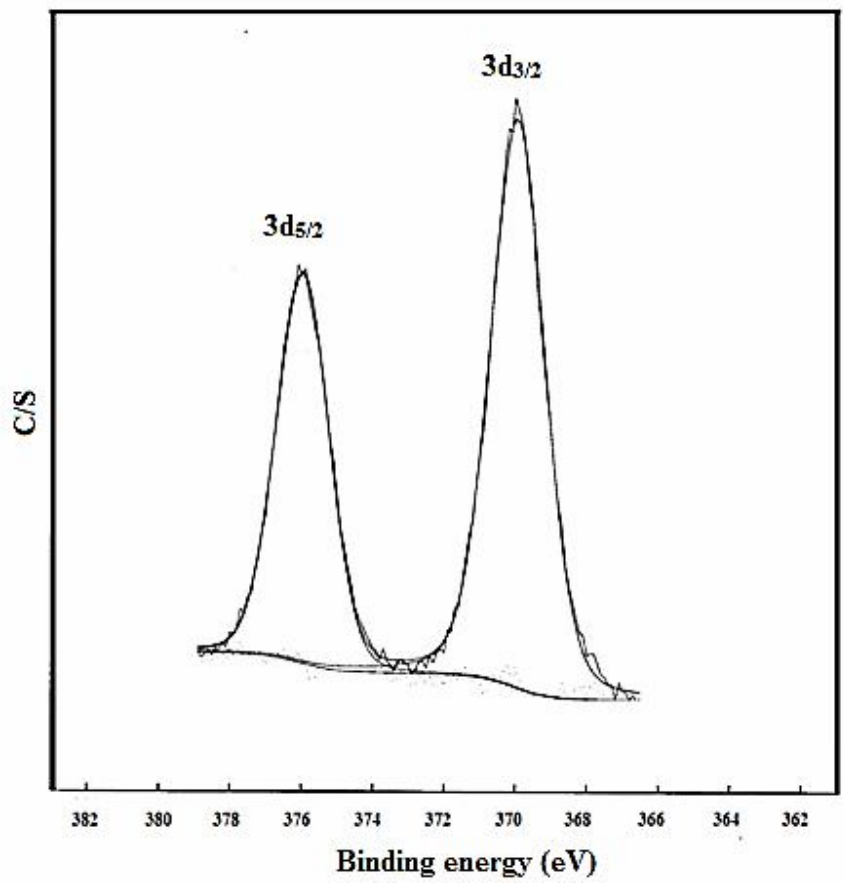

Fig. 5. XPS spectrum of PAA-Ag nanocomposite. The peaks are related to 3d metallic silver.

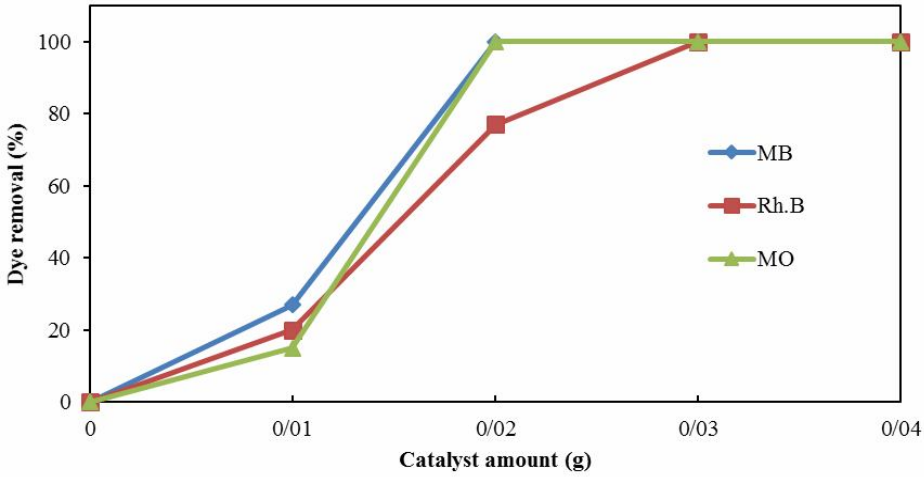

Fig. 6. Removal of dyes at different catalyst amount. The dyes are methylene blue (MB), methyl orange (MO), and rhodamine B (Rh. B).

core levels of silver, respectively. This and the energy splitting value of 3d doublet of silver about 6.0 eV confirm the formation of Ag NPs in metallic state [39,40].

Catalytic Degradation of Organic Dyes

The prepared PAA-Ag nanocomposite act as a catalyst facilitating electron transfer from the reduction agent (BH_4 anions) to dye molecules. When the molecules are being reduced, the colored water changes to colorless by-products or changes to the conjugated molecules due to degradation of dye molecules. The studies have demonstrated that removal of dyes in absence of catalyst has a low rate constant leading to the long term elimination of dye to several hours that is not suitable for practical applications [41]. However, by using an appropriate catalyst such as silver NPs distributed in a suitable porous matrix like PAA hydrogel, electron transfer process improves and the reduction reaction time decrease to a few min due to electron relay effect [30]. The removal of dyes by PAA and Ag-PAA in the presence of $NaBH_4$ was performed. The results showed the removal equals zero for PAA with $NaBH_4$ and Ag-PAA without $NaBH_4$. Therefore, the association of PAA on dye removal was zero. Due to results and our best of knowledge, the existence of Ag as an electron relay agent with $NaBH_4$ as a reducing agent is necessary to have the removal values more than zero.

In following, the effective factors in dye elimination such as the amount of catalyst, reaction time, dye initial concentration, and pH for the removal of dyes (MO, Rh. B and MB) with the help of BH4 by PAA-Ag catalyst are investigated. The amount of catalyst and concentration of dyes can affect the catalytic capacity. In addition, by varying pH, the surface charge of catalyst and the charge on dye molecules change, and consequently influence the swelling percentage of hydrogel. Then, these parameters impact the removal percentage of dyes [42-44]. Accordingly, these were selected to find optimum conditions for the removal of dyes.

Effect of the catalyst amount. Figure 6 illustrates the effect of catalyst amount on the removal percentage of dye at conditions: 50 ppm of each dye, 15 min reaction time, and 0.01 ppm of $NaBH_4$. The results showed that the amount of catalyst equal to 0.02 g completely removed the MO and MB dyes. In addition, 0.03 g of catalyst eliminated Rh. B dye by 100%. These amounts were used to remove dyes in the next experiments.

Effect of time factor. The effect of reaction time on degradation of dye is shown in Fig. 7. Degradation is displayed by a decrease in peak height of absorbance and absorption intensity at λ_{max} of dye. According to Fig. 7, a rapid decrease occurs in the major peak height of dyes in 12 minutes after adding PAA-Ag catalyst. When the peak height of dye at λ_{max} of dye is equal to zero, the dye was degraded completely. Figures 7a, b and c correspond to MO, Rh. B and MB spectrums of dyes, respectively.

Effect of dye concentration. Figure 8 demonstrates the removal of dyes at the different initial concentrations. Figures 8a, b and c correspond to MO, Rh. B and MB, respectively. The concentration of dyes was changed from 10 ppm to 50 ppm. According to Figs. 8a for 10 ppm of concentration, MO was removed during 10 min completely, and for 30 ppm of concentration, it was eliminated in 15 min with 100% of degradation. According to Fig. 8b, for 10 and 50 ppm of dye concentration, Rh. B was removed over 8 and 14 min by 100%, respectively. 10 and 50 ppm of MB were also removed during 8 and 12 min, respectively, as given in Fig. 8c.

Effect of pH. Figure 9 displays the effect of pH on the removal of dyes. The experiments were performed at pH equal to 2, 5, 6.5, 9 and optimum conditions documented in previous sections. As shown, for Rh. B, the removal of dye was a maximum value, 100% at pH = 6.5. The removal was negligible at other pHs. For MO dye at acidic Ph, equal to 2 and 5, the dye removal was 40% and 35%, respectively, and at pH = 9, it was negligible. MO was also removed completely at pH = 6.5. Furthermore, the removal of dye was 100% for MB dye at pH = 5 and 6.5, and it was negligible at other pHs.

Table 1 shows a comparison between the properties of the prepared catalyst and a similar catalyst by another approach to degrade the dyes. As shown, the selected approach in this study has exhibited excellent results against the other approaches.

CONCLUSIONS

In summary, PAA-Ag nanocomposite has been synthesized successfully and characterized by SEM, TEM,

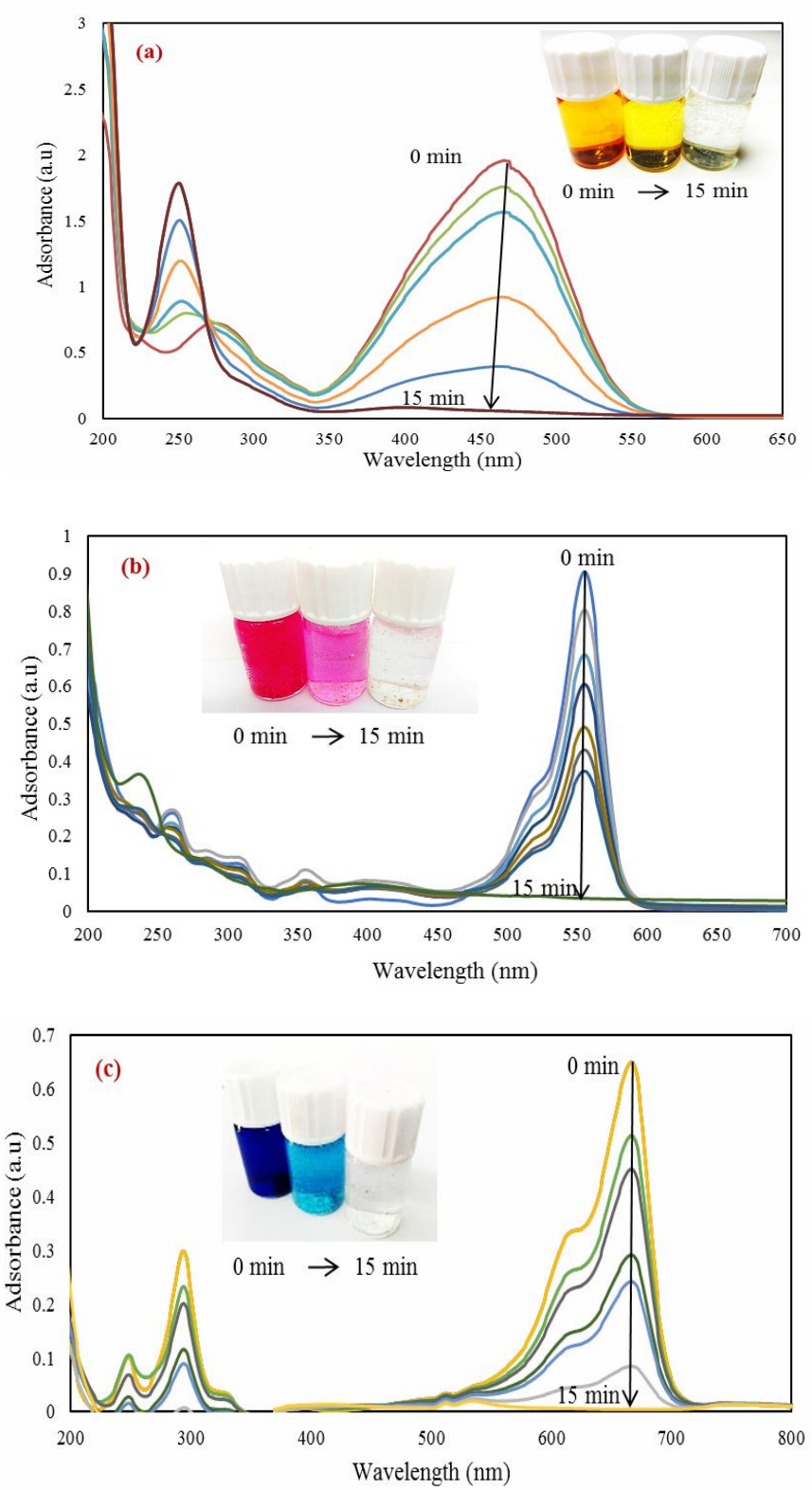

Fig. 7. Successive UV-Vis spectra of a) methyl orange (MO), b) rhodamine B (Rh. B), and c) methylene blue (MB) dye reduction, using PAA-Ag nanocomposite as the catalyst and $NaBH_4$ as the reducing agent.

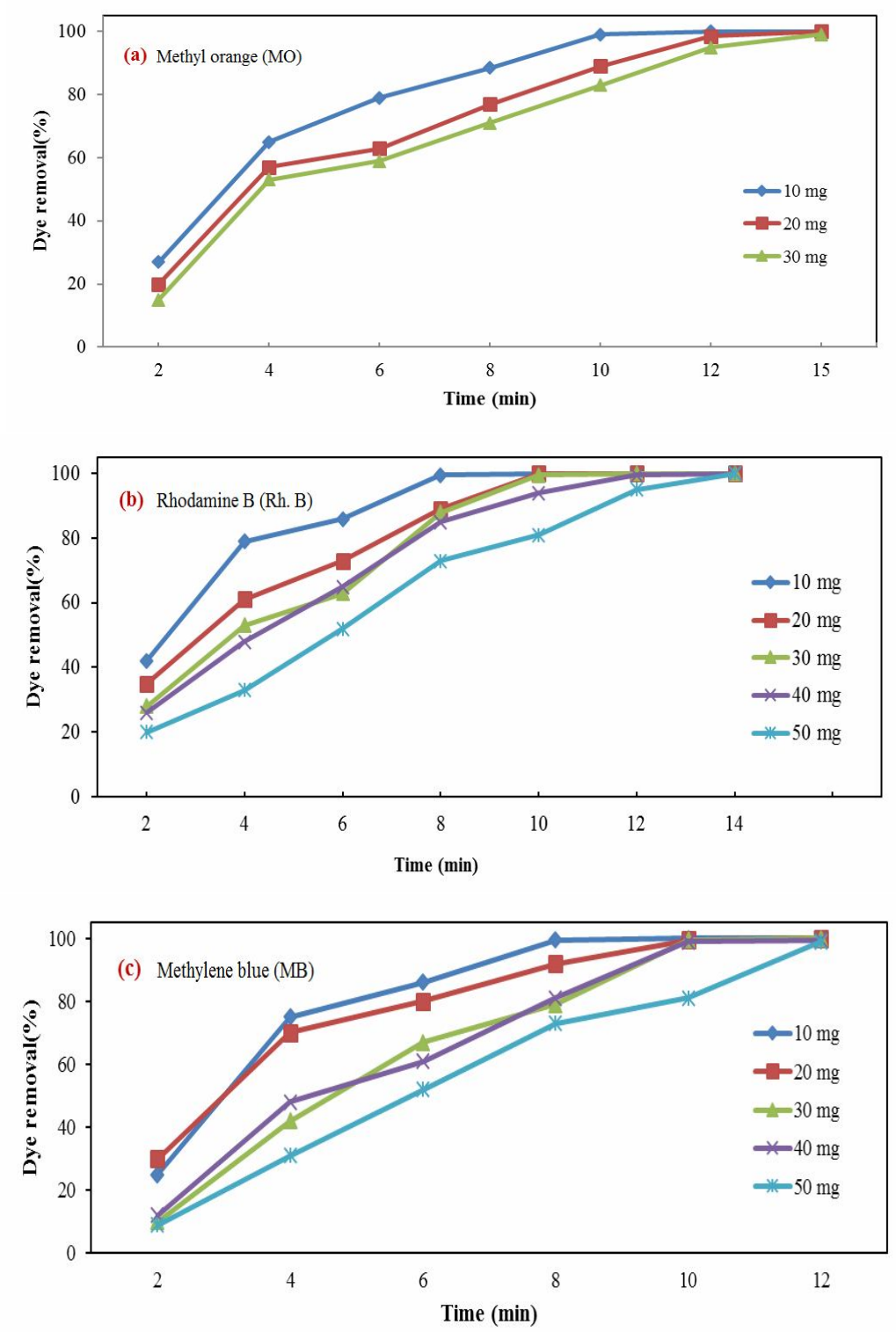

Fig. 8. Removal of dyes: a) methyl orange (MO), b) rhodamine B (Rh. B), and c) methylene blue (MB) at different initial concentrations from 10 to 50 ppm of concentration.

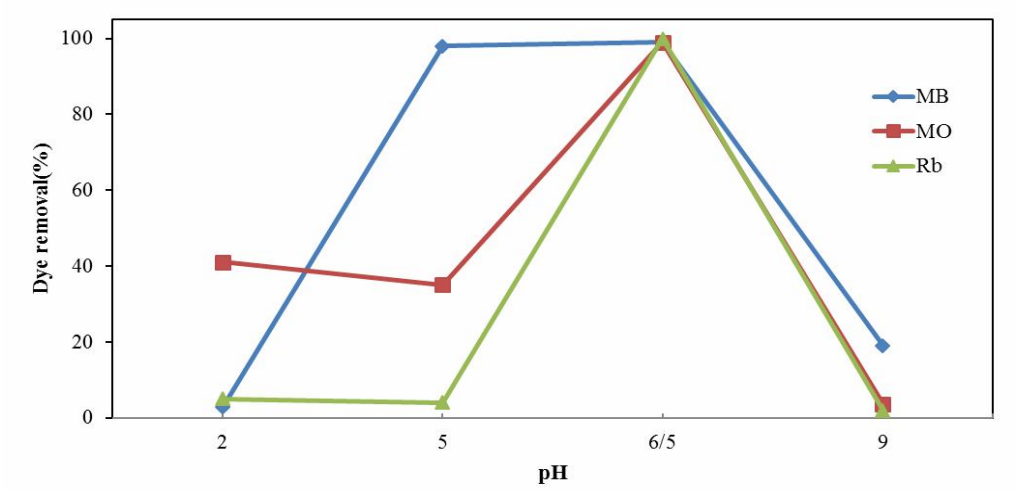

Fig. 9. Removal of dyes: a) methyl orange (MO), b) rhodamine B (Rh. B), and c) methylene blue (MB) at different pHs (pH = 2, 5, 6.5, and 9).

Table 1. A Comparison between Prepared Catalyst and a Similar Catalyst with another Approach

Type of catalyst	Dye	Concentration of dye	Size of NPs	Time	Removal percent	Amount of catalyst	Ref.
PAA-Ag/Ag NPs	Rh. B	4 ppm	10-15 nm	50 min	50%	1 ml (Volume)	Hou and *et al.*
	MB	10 ppm		90 min	60%		
	MO	-		-	-		
Ag-PAA nanocomposite	Rh. B	50 ppm	20-40 nm	<15 min	100%	0.03 g (Mass)	Current study
	MB	50 ppm			100%		
	MO	30 ppm			100%		

FT-IR, TGA, ICP and XPS. The catalyst has been used to degrade methyl orange (MO), rhodamine B (Rh. B) and methylene blue (MB) in water. The results illustrated that the amount of catalyst equal to 0.02 g with $NaBH_4$ (0.01 g) completely degrades MO and Rh. B. 0.03 g of catalyst degraded MB completely. The optimum conditions were pH = 6.5, reaction time less than 15 min, and initial concentration of 50 ppm for each dye with 0.01 g of $NaBH_4$. Furthermore, MB dye was completely degraded at pH = 5. Finally, the developed catalyst exhibited a satisfactory performance on degradation of organic dyes that could be applicable in wastewater purification purposes.

ACKNOWLEDGMENTS

The authors would like to thank from the "Clinical Research Development Center of Baqiyatallah hospital" for their kindly cooperation.

REFERENCES

[1] Aksu, Z., Application of biosorption for the removal of organic pollutants: a review. *Process Biochem.* **2005**, *40*, 997-1026. DOI: 10.1016/ j.procbio.2004.04.008

[2] Akar, S. T.; Özcan, A. S.; Akar, T.; Özcan, A.; Kaynak, Z., Biosorption of a reactive textile dye from aqueous solutions utilizing an agro-waste. *Desalination* **2009**, *249*, 757-761. DOI: 10.1016/ j.desal.2008.09.012

[3] Carmen, Z.; Daniela, S., Textile organic dyes-characteristics, polluting effects and separation/ elimination procedures from industrial effluents-a critical overview. In: Organic pollutants ten years after the Stockholm convention-environmental and analytical update, *In Tech.* **2012**. DOI: 10.5772/32373

[4] Dutta, P. K., An overview of textile pollution and its remedy. *Indian J. Env. Prot.* 1994, *14*, 443-446.

[5] Ponraj, M.; Gokila, K.; Zambare, V., Bacterial decolorization of textile Dye-Orange 3R. *Int. J. Adv. Biotechnol. Res.* **2011**, *2*, 168-177.

[6] Zollinger, H., Color chemistry: syntheses, properties, and applications of organic dyes and pigments. *JWS,* **2003**. DOI: 10.1002/anie.200385122.

[7] O'Neill, C.; Hawkes, F. R.; Hawkes, D. L.; Lourenço, N. D.; Pinheiro, H. M.; Delée, W., Color in textile effluents–sources, measurement, discharge consents and simulation: a review. *J. Chem. Technol. Biotechnol.* **1999**, *74*, 1009-1018. DOI: 10.1002/ (SICI)10974660(199911)74:11<1009:: AID-JCTB153>3.0.CO;2-N.

[8] Castillo-Carvajal, L. C.; Sanz-Martín, J. L.; Barragán-Huerta, B. E., Biodegradation of organic pollutants in saline wastewater by halophilic microorganisms: a review. *Environ. Sci. Pollut. Res. Int.* **2014**, *21*, 9578-9588. DOI: 10.1007/s11356-014-3036-z.

[9] Azin, E.; Moghimi, H.; Taheri, R. A., Development of carbon nanotube-mycosorbent for effective Congo red removal: optimization, isotherm and kinetic studies. *Desalin. Water Treat.* **2017**, *94*, 30-222. DOI: 10.5004/dwt.2017.21586.

[10] Meng, L.; Zhang, X.; Tang, Y.; Su, K.; Kong, J., Hierarchically porous silicon-carbon-nitrogen hybrid materials towards highly efficient and selective adsorption of organic dyes. *Sci. Rep.* **2015**, *5*, 7910. DOI: 10.1038/srep07910.

[11] Kazemi, F.; Mohamadnia, Z.; Kaboudin, B.; Karimi, Z., Photodegradation of methylene blue with a titanium dioxide/polyacrylamide photocatalyst under sunlight. *J. Appl. Polym. Sci.* **2016**, *133*. DOI: 10.1002/app.43386.

[12] Luo, S.; Duan, L.; Sun, B.; Wei, M.; Li, X.; Xu, A., Manganese oxide octahedral molecular sieve (OMS-2) as an effective catalyst for degradation of organic dyes in aqueous solutions in the presence of peroxymonosulfate. *Appl. Catal. B Environ.* **2015**, *164*, 92-99. DOI: 10.1016/j.apcatb.2014.09.008

[13] Kebria, M. R. S.; Jahanshahi, M.; Rahimpour, A., SiO_2 modified polyethyleneimine-based nanofiltration membranes for dye removal from aqueous and organic solutions. *Desalination.* **2015**, *367*, 255-264. DOI: 10.1016/j.desal.2015.04.017.

[14] Khansary, M. A.; Mellat, M.; Saadat, S. H.; Fasihi-Ramandi, M.; Kamali, M.; Taheri, R. A., An enquiry on appropriate selection of polymers for preparation of polymeric nanosorbents and nanofiltration/ ultrafiltration membranes for hormone micropollutants removal from water effluents. *Chemosphere.* **2017**, *168*, 91-9. DOI: 10.1016/ j.chemosphere.2016.10.049.

[15] Tian, Y.; Ju, B.; Zhang, S.; Hou, L., Thermoresponsive cellulose ether and its flocculation behavior for organic dye removal. *Carbohydr. Polym.* **2016**, *136*, 1209-1217. DOI: 10.1016/ j.carbpol.2015.10.031.

[16] Brillas, E.; Martínez-Huitle, C. A., Decontamination of wastewaters containing synthetic organic dyes by electrochemical methods. A general review. *Appl. Catal. B Environ.* **2015**, *166*, 603-643. DOI: 10.1016/ j.apcatb.2008.09.017.

[17] Labiadh, L.; Oturan, M. A.; Panizza, M.; Hamadi, N. B.; Ammar, S., Complete removal of AHPS synthetic dye from water using new electro-fenton oxidation catalyzed by natural pyrite as heterogeneous catalyst. *J. Hazard. Mater.* **2015**, *297*, 34-41. DOI: 10.1016/ j.jhazmat.2015.04.062.

[18] Bueno, P. D. L. C.; Gillerman, L.; Gehr, R.; Oron, G.,

Nanotechnology for sustainable wastewater treatment and use for agricultural production: A comparative long-term study. *Water Res.* **2017**, *110*, 66-73. DOI: 10.1016/j.watres.2016.11.060.

[19] Barton, L. E.; Auffan, M.; Durenkamp, M.; McGrath, S.; Bottero, J. Y.; Wiesner, M. R., Monte Carlo simulations of the transformation and removal of Ag, TiO_2, and ZnO nanoparticles in wastewater treatment and land application of biosolids. *Sci. Total Environ.* **2015**, *511*, 535-543. DOI: 10.1016/ j.scitotenv.2014.12.056.

[20] Sadegh, H.; Ali, G. A.; Gupta, V. K.; Makhlouf, A. S. H.; Shahryari-ghoshekandi, R.; Nadagouda, M. N.; Sillanpää, M.; Megiel, E., The role of nanomaterials as effective adsorbents and their applications in wastewater treatment. *J. Nanostruct. Chem*. **2017**, *7*, 1-14. DOI: 10.1007/s40097-017-0219-4.

[21] Santhosh, C.; Velmurugan, V.; Jacob, G.; Jeong, S. K.; Grace, A. N.; Bhatnagar, A., Role of nanomaterials in water treatment applications: a review. *Chem. Eng. J.* **2016**, *306*, 1116-1137. DOI: 10.1016/j.cej.2016.08.053.

[22] Nantaphol, S.; Chailapakul, O.; Siangproh, W., Sensitive and selective electrochemical sensor using silver nanoparticles modified glassy carbon electrode for determination of cholesterol in bovine serum. *Sens. Actuators B Chem.* **2015**, *207*, 193-198. DOI: 10.1016/j.snb.2014.10.041.

[23] Li, D.; Yu, S.; Sun, C.; Zou, C.; Yu, H.; Xu, K., U-shaped fiber-optic ATR sensor enhanced by silver nanoparticles for continuous glucose monitoring. *Biosens. Bioelectron.* **2015**, *72*, 370-375. DOI: 10.1016/j.bios.2015.05.023.

[24] Hu, D.; Lin, J.; Jin, S.; Hu, Y.; Wang, W.; Wang, R.; Yang, B., Synthesis, structure and optical data storage properties of silver nanoparticles modified with azobenzene thiols. *Mater. Chem. Phys.* **2016**, *170*, 108-112. DOI: 10.1016/j.matchemphys.2015.12.025.

[25] Franci, G.; Falanga, A.; Galdiero, S.; Palomba, L.; Rai, M.; Morelli, G.; Galdiero, M., Silver nanoparticles as potential antibacterial agents. *Molecules* **2015**, *20*, 8856-8874. DOI: 10.3390/ molecules20058856.

[26] Agnihotri, S.; Mukherji, S.; Mukherji, S., Size-controlled silver nanoparticles synthesized over the range 5-100 nm using the same protocol and their antibacterial efficacy. *Rsc Adv.* **2014**, *4*, 3974-3983. DOI: 10.1039/C3RA44507K.

[27] Bhakya, S.; Muthukrishnan, S.; Sukumaran, M.; Muthukumar, M.; Kumar, S. T.; Rao, M., Catalytic degradation of organic dyes using synthesized silver nanoparticles: a green approach. *J. Bioremediat. Biodegrad.* **2015**, *6*, 1. DOI: 10.4172/2155-6199.1000312.

[28] Vidhu, V.; Philip, D., Catalytic degradation of organic dyes using biosynthesized silver nanoparticles. *Micron.* **2014**, *56*, 54-62. DOI: 10.1016/ j.micron.2013.10.006.

[29] Joseph, S.; Mathew, B., Microwave-assisted green synthesis of silver nanoparticles and the study on catalytic activity in the degradation of dyes. *J. Mol. Liq*. **2015**, *204*, 184-191. DOI: 10.1016/ j.molliq.2015.01.027.

[30] Gupta, V.; Singh, H. P.; Sharma, R. K., Metal nanoparticles with high catalytic activity in degradation of methyl orange: An electron relay effect. *J. Mol. Catal. A Chem.* **2011**, *335*, 248-252. DOI: 10.1016/j.molcata.2010.12.001.

[31] Falletta, E.; Bonini, M.; Fratini, E.; Lo Nostro, A.; Becheri, A.; Lo Nostro P.; Baglioni, P., Poly(acrylic) acid-coated silver nanoparticles for antibacterial textile finishing. *Nanotech* **2007**, *4*, 412-414. ISBN: 1-4200-6376-6.

[32] Iravani, S.; Korbekandi, H.; Mirmohammadi, S.; Zolfaghari, B., Synthesis of silver nanoparticles: chemical, physical and biological methods. *Res. Pharm. Sci.* **2014**, *9*, 385.

[33] Logeswari, P.; Silambarasan, S.; Abraham, J., Synthesis of silver nanoparticles using plants extract and analysis of their antimicrobial property. *J. Saudi Chem, Soc.* **2015**, *19*, 311-317. DOI: 10.1016/ .jscs.2012.04.007.

[34] Park, S.; Cha, S. H.; Cho, I.; Park, S.; Park, Y.; Cho, S.; Park, Y., Antibacterial nanocarriers of resveratrol with gold and silver nanoparticles. *Mater. Sci. Eng. C.* **2016**, *58*, 1160-1169. DOI: 10.1016/j.msec.

[35] Ghavami Nejad, A.; Park, C. H.; Kim, C. S., *In situ* synthesis of antimicrobial silver nanoparticles within

antifouling zwitterionic hydrogels by catecholic redox chemistry for wound healing application. *Biomacromolecules.* **2016**, *17*, 1213-1223. DOI: 10.1021/acs.biomac.6b00039.

[36] Reithofer, M. R.; Lakshmanan, A.; Ping, A. T.; Chin, J. M.; Hauser, C. A., *In situ* synthesis of size-controlled, stable silver nanoparticles within ultrashort peptide hydrogels and their anti-bacterial properties. *Biomaterials.* **2014**, *35*, 7535-7542. DOI: 10.1016/ j.biomaterials.

[37] Liang, M.; Su, R.; Huang, R.; Qi, W.; Yu, Y.; Wang, L.; He, Z., Facile in situ synthesis of silver nanoparticles on procyanidin-grafted eggshell membrane and their catalytic properties. *ACS Appl. Mater. Interfaces.* **2014**, *6*, 4638-4649. DOI: 10.1021/ am500665p. Epub.

[38] Demirci, S.; Sahiner, N., The use of metal nanoparticle-embedded poly(ethyleneimine) composite microgel in the reduction of nitrophenols. *Water Air. Soil. Pollut.* **2015**, *226*, 64. DOI: 10.1007/ s11270-015-2332-7.

[39] Patwadkar, M. V.; Gopinath, C. S.; Badiger, M. V.; An efficient Ag-nanoparticle embedded semi-IPN hydrogel for catalytic applications. *RSC Adv.* **2015**, *5*, 7567. DOI: 10.1039/C4RA14594A.

[40] Akhavan, O.; Abdolahad, M.; Abdi, Y.; Mohajerzadeh, S., Silver nanoparticles within vertically aligned multi-wall carbon nanotubes with open tips for antibacterial purposes. *J. Mater. Chem.* **2011**, *2*1, 387. DOI: 10.1039/C0JM02395G.

[41] Ghosh, S. K.; Kundu, S.; Mandal, M.; Pal, T., Silver and gold nanocluster catalyzed reduction of methylene blue by arsine in a micellar medium. *Langmuir.* **2002**, *18*, 8756-8760. DOI: 10.1021/ la0201974.

[42] Hou, C.; Ma, K.; Jiao, T.; Xing, R.; Li, K.; Zhoub, J.; Zhang, L., Preparation and dye removal capacities of porous silver nanoparticle containing composite hydrogels *via* poly (acrylic acid) and silver ions. RSC.

[43] Boruah, M.; Gogoi, P.; Manhar, A. K.; Khannam, M.; Mandal, M.; Dolui, S. K., Biocompatible carboxymethylcellulose-g-poly(acrylic acid)/OMMT nanocomposite hydrogel for in vitro release of vitamin B_{12}. *RSC Adv.* **2014**, *4*, 43865-43873. DOI: 10.1039/C4RA07962K.

[44] Hamidi, M.; Azadi, A.; Rafiei, P., Hydrogel nanoparticles in drug delivery. *Adv. Drug Deliver. Rev.* **2008**, *60*, 1638-1649. DOI: 10.1016/ j.addr.2008.08.002.

[45] Adv. 2014, 00, 1-3. DOI: 10.1039/x0xx00000x.